Wang *et al. EPJ Techniques and Instrumentation* (2016) 3:3
DOI 10.1140/epjti/s40485-016-0030-5

EPJ Techniques and Instrumentation
a SpringerOpen Journal

RESEARCH ARTICLE Open Access

Fabrication of ion-trap electrodes by self-terminated electrochemical etching

Zhao Wang[1,2,3], Le Luo[2*], Karthik Thadasina[2,4], Kim Qian[2,4], Jinming Cui[1,3] and Yunfeng Huang[1,3]

*Correspondence: leluo@iupui.edu
[2]Department of Physics, Indiana University Purdue University Indianapolis, 46202 Indianapolis, IN, USA
Full list of author information is available at the end of the article

Abstract
Self-terminated electrochemical etching is applied to fabricate needle electrodes for ion traps. We study the surface morphology of the electrodes with scanning electron microscopy and atomic force microscopy, and find that the surface curvature and roughness can be reduced by optimizing the etching parameters. Our method provides a convenient and low-cost solution to improve the surface quality of electrodes for ion traps.

Keywords: Ion trap, Electrochemical etching, Surface roughness

Introduction

Needle electrode is one of the most common geometries of electrodes used in Paul traps for trapped ion quantum information processing (QIP) [1–10]. As examples, three different Paul traps, including the 3-fork needle trap [10], the "tack" trap [5], and the linear Paul trap [11], are shown in Fig. 1, where needle electrodes generate either radio-frequency (rf) or DC voltages for ion trapping. It is highly desired to minimize surface roughness of these needle electrodes, because a rough surface could contribute to anomalous heating of ion. Such hearing is usually much higher than the thermal Johnson noise [12]. Anomalous heating not only reduces the trapping lifetime of ions, but also limits the fidelity of quantum gate operations [13–17]. Currently such anomalous heating is a major obstacle to scalable trapped ion QIP.

In practice, anomalous heating can be suppressed either by cleaning surface or reducing surface roughness [12, 16, 18, 19]. Surface roughness is characterized by parameters including the root-mean-square roughness, the maximum roughness depth, and the mean spacing of the local peaks of the profile [20]. Reducing surface roughness results in a more uniform work function and less surface contamination, which helps to reduce the electrical noise from the surface [12]. Currently state-of-the-art surface processing techniques are able to reduce the surface roughness to nanometer level [21–30], but these techniques usually requires the specialized equipments of surface science, which are too complicated for most ion trap research groups.

Instead, electrochemical etching has been used as a convenient technique to improve the surface quality for various applications. Previously, a high-speed computer-controlled circuit was used to control the speed and time of electrochemical etching, enabling fabricating high surface quality metal tips for scanning tunneling microscopy (STM) [31–35].

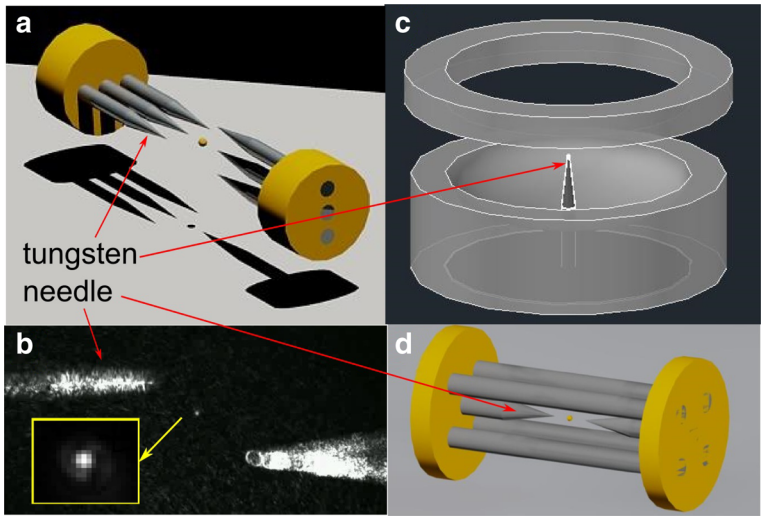

Fig. 1 Needle electrodes are used in different types of the Paul traps for trapped ion quantum information. **a** The 3-fork needle trap used by our IUPUI-USTC group. **b** A single $^{171}Yb^{+}$ trapped in **a**). **c** The "tack" trap [5]. **d** The four-rod linear traps [11]

It is interesting to study if controllable etching process can also be used for the fabrication of ion-trap electrodes to improve the surface quality. However, the etching procedure used for the STM tips can not be applied to the ion-trap electrodes directly, because the ion-trap electrodes have very different geometries comparing with the STM ones. As shown in Fig. 2, the STM tip has a rapid decrease in curvature over a short distance which is required by surface probing, while the needle electrode prefers a long and gradual taper towards the apex which helps to reduce the fluctuation in the surface electric field. Here we present a self-terminated electrochemical etching technique for ion-trap needle electrodes, which can produce smooth surface with a large (1000:1) length-to-width aspect ratio.

Setup and procedure

Our experimental setup is shown in Fig. 3. Sodium hydroxide solution (NaOH, 400 ml of 2 mol/L) is used to etch a tungsten rod. The tungsten rod can be moved vertically

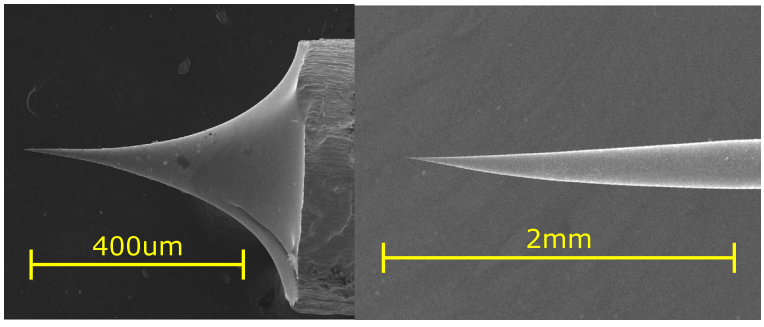

Fig. 2 The comparison between the STM tip and the ion-trap needle electrode. *Left*: STM tips are short and sharp for nano-scale surface probing. *Right*: Ion-trap needle electrodes are long and smooth for reducing the fluctuation of the electrical field

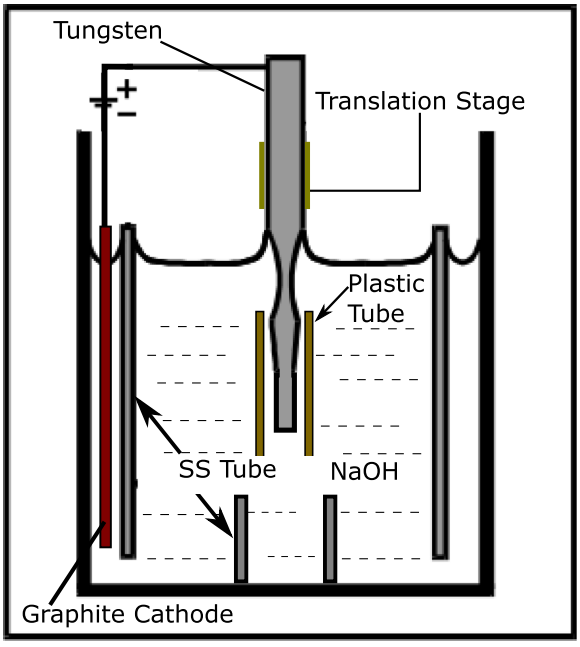

Fig. 3 The self-terminated electrochemical etching setup. The tungsten rod is immersed into NaOH solution as anode and can be moved vertically by a computer-controlled translation stages. Two stainless steel (SS) tubes are placed in the beaker, where the larger one produces an etching electric field with circular symmetry, and the small one protects the down-piece when the rod separates into two pieces. The plastic tube surrounding to the down-piece is used to suppress the etching reaction

by a computer-controlled translation stage. The etching process separates the tungsten rod into two pieces: the up-piece and down-piece. When the process ends, the down-piece falls to the bottom of the beaker. We find that the etched tips of the up-piece and down-piece have quite different profiles. While the up-piece has a sharp tip profile due to the surface tension of the solution, the down-piece has a tapering tip profile with a large length-to-width aspect ratio [33], which is more suitable for the needle-electrode. We also notice that the freshly-etched metal surface of the down-piece is preserved in the solution, while the etched surface of the up-piece will be oxidized in the air. Based on these findings, we use the down-piece as needle-electrodes for all our experiments.

The tungsten rod is connected to the positive pole of a power supply with the maximum output of 30 V and 3 A. There are two stainless steel (SS) tubes placed in the beaker. By placing the graphite cathode outside the large SS tube, we prevent the tungsten rod from the electrolyte turbulence. The smaller SS tube is used to protect the down-piece when it falls down. We also use a non-reactive plastic tube to control the etching speed. Inside the plastic tube, the etching speed is significantly suppressed. We adjust the etching length of the electrode by varying the length of the rod in and out of the plastic tube. With this design, the etching speed can be adjusted, allowing us to fabricate the electrodes with controllable length-to-diameter ratios.

The chemical reactions for electrochemical etching of tungsten with sodium hydroxide are described by [36]:

Cathode: $6H_2O + 6e^- \rightarrow 3H_{2(g)} + 6OH^-$,

Anode: $W_{(s)} + 8OH^- \rightarrow WO_4^{2-} + 4H_2O + 6e^-$, and

Overall: $W_{(s)} + 2OH^- + 2H_2O \rightarrow WO_4^{2-} + 3H_{2(g)}$.

This etching process is self-terminated when the tungsten rod necks at solution surface and separates into two pieces [35].

A typical experimental procedure is described as follows. We first mill and polish the tungsten rod to a right size. Then the rod surface is pre-cleaned by sodium hydroxide solution. The tungsten rod is carefully aligned so that it is perpendicular to the solution surface. We adjust the length immersed into solution so that it is slightly longer than the desired electrode length (e.g. 42 mm rod immersed into solution for 41 mm long electrode). After the etching starts, we adjust the position of the plastic tube to control the etching speed. In the end, the rod is etched into two pieces and the down-piece falls, which self-terminates the etching process. The down-piece is then taken out and washed by distill water before it is stored in an argon gas box. The argon gas prevents the freshly-etched surface of the needle electrode from oxidizing. Following the fabrication, we use scanning electron microscopy (SEM) and atomic force microscopy (AFM) to study the dependence of surface morphology on the etching parameters.

When implementing the above procedure, we find that a few things are crucial to fabricate electrodes with high surface quality. It is important to keep the tungsten rod exactly perpendicular to the solution surface and in the the center of the larger SS tube. Otherwise, the tip profile will no longer have cylindrical symmetry. For translating the rod during the etching process, it is required to pull the tungsten rod up instead of pushing-down because pushing-down will result in the multi-level etching on the down-piece. By pulling up, the multi-level structure only appears on the up-piece shown in Fig. 4.

Result and discussion

Etching parameters, such as temperature, voltage, solution concentration, metal purity, immersion depth, and environmental vibration, determine the profile and surface roughness of needle electrodes. Here we adopt the trial-and-error method to optimize these parameters. We first fabricate more than 200 electrodes with different etching parameters. We then use optical microscopy and SEM to image the surface profiles, shown in

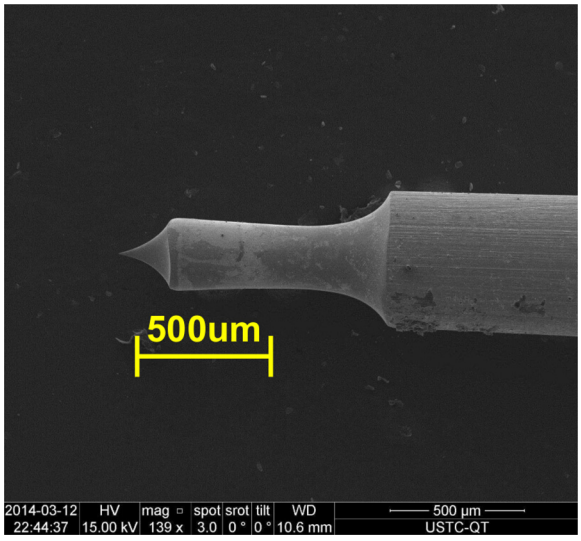

Fig. 4 The multi-level etching developed on the up-tip. The right side narrowing corresponds to the initial position of the solution surface and the left side tip to the final position of the solution surface

Fig. 5 with typical images. After that, the specification of surface roughness is recorded by AFM. By studying the dependence of the surface roughness on the etching parameters, we optimize the etching process to reduce the surface roughness. The detailed effects of individual etching parameters are summarized below.

Etching voltage

The current density vs. voltage (j - V) curve of a specific electrochemical etching process (a 0.5 mm diameter rod with a immersion depth of 40 mm in 2 mol/L NaOH solution) is shown in Fig. 6. For different etching voltages, the specifications of the surface roughness with Ra (arithmetic average of absolute values), Rq (root mean squared), and Rt (Maximum Height of the Profile) are shown in Table 1. We find that Zone I in Fig. 6 represents the direct dissolution of the anode, known as regular etching. Zone II represents the formation of a passivated layer on the anode surface, where the current saturates as the voltage increases due to the diffusion of anode atoms into the passivated layers. Zone III is the polishing zone where the passivated layer stabilizes, where the bulges on the surface have higher local electric fields and are easily dissolved by the solution. We verify that Zone III is the ideal region to minimize the surface roughness [37, 38]. As shown in Fig. 6, the maximum voltage in Zone III is 6 V, where we find that the surface roughness is reduced significantly with Ra 6.63 nm, Rq 8.72 nm, and Rt 67.8 nm respectively. In Zone IV, the passivated layer starts to break down, and oxygen become visible on the anode ($2H_2O \rightarrow 4H^+ + O_{2(g)} + 4e^-$). Due to the formation of oxygen bubbles, the surface becomes much more rough with the appearance of pits. Finally, at the high voltage side of Zone IV, the electrolyte solution begins to decompose and turbulence develops in the solution, where the etching process becomes uncontrollable.

For tungsten rods with different diameters, the optimal etching voltage changes slightly: the larger diameter rods have the larger optimal voltage. We have tested rods with diameters at 0.5 mm, 1 mm, 1.6 mm, 2.0 mm, 2.4 mm, and 4.0 mm. We find that one can start

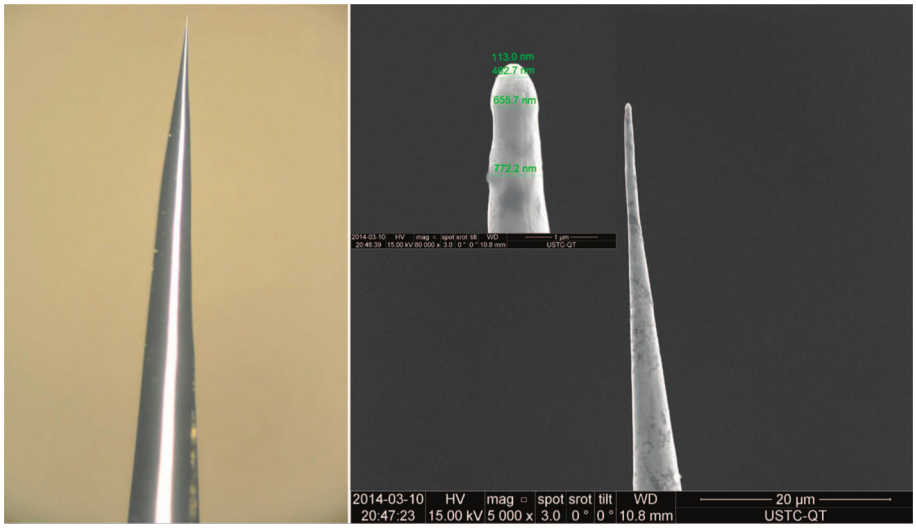

Fig. 5 The tungsten tip images. The left optical image is from an optical microscope with 500x magnification. The right SEM image has the 5000x magnification and the embedded one has a 80000x magnification

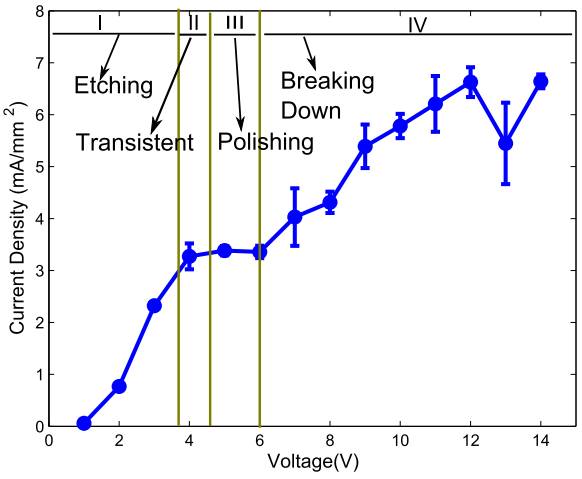

Fig. 6 The current density versus voltage curve for electrochemical etching the tungsten rods (0.5 mm diameter and 40 mm immersion depth). The blue curve is the average current density versus the etching voltage. The etching process are divided into four zones. Zone I shows very rough surface and Zone II shows a transition stage where the surface evolves from rough to smooth. Zone III is our targeting region where the tungsten electrodes show very smooth surfaces after etching. In Zone IV, the electrolyte solution begins to breakdown and fluid turbulence appears

at 6.0 V for 0.5 mm diameter, and then increase voltage gradually to locate the optimal etching voltage for the larger diameter rods.

Immersion depth

The dependence of etching current on the immersion depth is almost linear in Zone III and logarithmic in Zones I and II, as shown in Fig. 7. This relation can be explained as follows: In the polishing region of Zone III, the surface is very smooth so that the current density is constant, resulting in a linear relation between the total current and the immersion depth. For the lower voltage, the electrode has surface defects accumulated against the diffusion of electrons and ions, and the dependence of the current on the immersion depth is not linear any more.

Solution concentration

The lower solution concentration has higher resistance and thus increases the optimal etching voltage. The solution of higher concentration results in the formation

Table 1 The dependence of surface roughness on the etching voltages

Voltage(V)	Ra(nm)	Rq(nm)	Rt(nm)
1	145	183	1096
2	88.9	116	964
3	40.5	50.9	375
4	18.8	24.8	171
5	17.3	22.4	189
6	6.63	8.72	67.8
7	9.6	16.0	246
8	47	63.8	1787
10	182	255	2086
12	110	143	988
14	306	376	1728

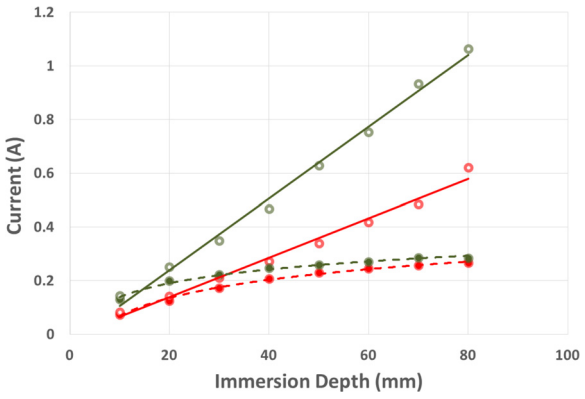

Fig. 7 The dependence of etching current on the immersion depth. The red open circles are measurements of 0.5 mm rods with 7 V etching voltage. The green open circles corresponds 1.0 mm rods with 7 V. The red solid dots corresponds 0.5 mm rods with 3 V. The green solid circles corresponds 1 mm rods with 3V. The fitted curves for 7V are linear while the fitted curves for 3V are logarithmic

of crystallites on the anodes, which increases the surface roughness. To reduce surface roughness, the concentration of electrochemical fluid is around 2 mol/L in our experiments.

Protection tube

The larger stainless steel tube acts as a shield cathode surrounding the tungsten electrode. Due to its cylindrical symmetry, the electric field is also cylindrical, making the etching on the rod cylindrically symmetric. This tube also help to keep the solution at rest near the anode region. We find keep cylindrical symmetry is important during the whole etching process. Once the symmetry is broken, the etching process will no longer be isotropic, leading to an irregular geometric profile of the electrode.

Rod surface

The initial rod surface roughness is also important to the final surface roughness after etching. The commercial tungsten electrodes are chemically pure (e.g. pure tungsten from McMaster-Carr # 8000A511). Because of the existed oxidization layers, the surface of these rods needs to be cleaned before the formal electrochemical etching. These oxidization layers can be dissolved by immersing them in sodium hydroxide solution for 1 minute and then cleaning the residue with distilled water.

Conclusion

The fabricated needle electrodes have been used to make a 3-fork needle trap, shown in Fig. 1(a) for our trapped ion experiments [10]. The trapping life-time is 24 hours averagely for a single trapped ion. In summary, we present a convenient and self-terminated electrochemical etching method to fabricate needle electrodes for ion trap. By studying the surface roughness dependence on the etching parameters using different imaging techniques, we have verified that the optimized etching parameters can reduce the surface roughness of electrodes significantly.

Competing interests
The authors declare that they have no competing interests.

Authors' contributions
ZW carried out the electrode fabrication, imaging taking and analysis, participated in experiment design, and drafted the manuscript. KT and KQ participated in the experiment. JC participated in the experiment design. LL participated in designing the fabrication, experimental studies, and drafting the manuscript. HYF provides suggestions to the experiments and helped ZW to setup. Y-F. H. and L.L supervised the project. All authors read and approved the final manuscript.

Acknowledgements
LL is a member of the Indiana University Center for Spacetime Symmetries (IUCSS). LL thanks the support from Indiana University Research Support Funds Grant (RSFG) and Faculty Award from Purdue University Purdue Research Foundation (PRF). HYF thanks the support from the National Basic Research Program of China (2011CB921200), and the National Science Fund of China for Distinguished Young Scholars (61225025).

Author details
[1]Key Lab of Quantum Information, CAS, University of Science and Technology of China, 230026 Hefei, Anhui, China. [2]Department of Physics, Indiana University Purdue University Indianapolis, 46202 Indianapolis, IN, USA. [3]Synergetic Innovation Center of Quantum Information & Quantum Physics, University of Science and Technology of China, 230026 Hefei, Anhui, China. [4]Carmel High School, 46032 Carmel, IN, USA.

Received: 1 September 2015 Accepted: 3 March 2016
Published online: 17 March 2016

References

1. Deslauriers L, Olmschenk S, Stick D, Hensinger WK, Sterk J, Monroe C (2006) Scaling and suppression of anomalous heating in ion traps. Phys Rev Lett 97:103007
2. Olmschenk S, Younge KC, Moehring DL, Matsukevich DN, Maunz P, Monroe C (2007) Manipulation and detection of a trapped Yb^+ hyperfine qubit. Phys Rev A 76:052314
3. Blatt R, Wineland D (2008) Entangled states of trapped atomic ions. Nature 453(7198):1008–1015
4. Luo L, Hayes D, Manning TA, Matsukevich DN, Maunz P, Olmschenk S, Sterk JD, Monroe C (2009) Protocols and techniques for a scalable atom-photon quantum network. Fortschritte der Physik 57(11-12):1133–1152
5. Shu G, Chou CK, Kurz N, Dietrich MR, Blinov BB (2011) Efficient fluorescence collection and ion imaging with the "tack" ion trap. JOSA B 28(12):2865–2870
6. Sterk JD, Luo L, Maunz P, Manning TA, Monroe C (2012) Photon collection from a trapped ion-cavity system. Phys Rev A 85:062308
7. Steiner M, Meyer HM, Deutsch C, Reichel J, Köhl M (2013) Single ion coupled to an optical fiber cavity. Phys Rev Lett 110(4):043003
8. Hoffman MR, Noel TW, Auchter C, Jayakumar A, Williams SR, Blinov BB, Fortson E (2013) Radio-frequency-spectroscopy measurement of the landé g_j factor of the $5\mathrm{D}_{5/2}$ state of Ba^+ with a single trapped ion. Phys Rev A 88(2):025401
9. Meyer HM, Stockill R, Steiner M, Le Gall C, Matthiesen C, Clarke E, Ludwig A, Reichel J, Atatüre M, Köhl M (2015) Direct photonic coupling of a semiconductor quantum dot and a trapped ion. Phys Rev Lett 114:123001
10. Cui JM, Huang YF, Wang Z, Cao DY, Wang J, Lv WM, Lu Y, Luo L, del Campo A, Han YJ, Li CF, Guo GC (2015) Supporting Kibble-Zurek Mechanism in Quantum Ising Model through a Trapped Ion. arXiv:1505.05734
11. Madsen MJ (2006) Advanced ion trap development and ultrafast laser-ion interactions. PhD thesis, University of Michigan
12. Hite D, Colombe Y, Wilson A, Allcock D, Leibfried D, Wineland D, Pappas D (2013) Surface science for improved ion traps. MRS Bull 38(10):826–833
13. Chiaverini J, Sage J (2014) Insensitivity of the rate of ion motional heating to trap-electrode material over a large temperature range. Phys Rev A 89(1):012318
14. Eltony AM, Park HG, Wang SX, Kong J, Chuang IL (2014) Motional heating in a graphene-coated ion trap. Nano Lett 14(10):5712–5716
15. Turchette Q, King B, Leibfried D, Meekhof D, Myatt C, Rowe M, Sackett C, Wood C, Itano W, Monroe C, et al. (2000) Heating of trapped ions from the quantum ground state. Phys Rev A 61(6):063418
16. Hite D, Colombe Y, Wilson A, Brown K, Warring U, Jördens R, Jost J, McKay K, Pappas D, Leibfried D, et al. (2012) 100-fold reduction of electric-field noise in an ion trap cleaned with in situ argon-ion-beam bombardment. Phys Rev Lett 109(10):103001
17. Ospelkaus C, Warring U, Colombe Y, Brown K, Amini J, Leibfried D, Wineland D (2011) Microwave quantum logic gates for trapped ions. Nature 476(7359):181–184
18. Allcock D, Guidoni L, Harty T, Ballance C, Blain M, Steane A, Lucas D (2011) Reduction of heating rate in a microfabricated ion trap by pulsed-laser cleaning. New J Phys 13(12):123023
19. McKay K, Hite D, Colombe Y, Jördens R, Wilson A, Slichter D, Allcock D, Leibfried D, Wineland D, Pappas D (2014) Ion-trap electrode preparation with Ne^+ bombardment. arXiv:1406.1778
20. Bennett JM, Mattsson L (1999) Introduction to Surface Roughness and Scattering. 2nd edn. Optical Society of America, Washington D.C.
21. Binnig G, Rohrer H, Gerber C, Weibel E (1982) Surface studies by scanning tunneling microscopy. Phys Rev Lett 49(1):57
22. Stupian GW, Leung MS (1989) A scanning tunneling microscope based on a motorized micrometer. Rev Sci Instrum 60(2):181–185
23. Lemke H, Göddenhenrich T, Bochem H, Hartmann U, Heiden C (1990) Improved microtips for scanning probe microscopy. Rev Sci Instrum 61(10):2538–2541

24. Musselman I, Peterson P, Russell P (1990) Fabrication of tips with controlled geometry for scanning tunnelling microscopy. Precis Eng 12(1):3–6
25. Biegelsen D, Ponce F, Tramontana J, Koch S (1987) Ion milled tips for scanning tunneling microscopy. Appl Phys Lett 50(11):696–698
26. Vasile M, Grigg D, Griffith J, Fitzgerald E, Russell P (1991) Scanning probe tip geometry optimized for metrology by focused ion beam ion milling. J Vac Sci Technol B 9(6):3569–3572
27. Fink HW (1986) Mono-atomic tips for scanning tunneling microscopy. IBM J Res Dev 30(5):460–465
28. Akama Y, Nishimura E, Sakai AS, Murakami H (1990) New scanning tunneling microscopy tip for measuring surface topography. J Vac Sci Technol A 8(1):429–433
29. Yamamura K, Takiguchi T, Ueda M, Deng H, Hattori A, Zettsu N (2011) Plasma assisted polishing of single crystal sic for obtaining atomically flat strain-free surface. CIRP Ann Manuf Technol 60(1):571–574
30. Kumar G, Staffier PA, Blawzdziewicz J, Schwarz UD, Schroers J (2010) Atomically smooth surfaces through thermoplastic forming of metallic glass. Appl Phys Lett 97(10):101907
31. Chen Y, Xu W, Huang J (1989) A simple new technique for preparing stm tips. J Phys E Sci Inst 22(7):455–457
32. Ibe JP, Bey PP, Brandow SL, Brizzolara RA, Burnham NA, DiLella DP, Lee KP, Marrian CRK, Colton RJ (1990) On the electrochemical etching of tips for scanning tunneling microscopy. J Vac Sci Technol A 8(4):3570–3575
33. Melmed AJ (1991) The art and science and other aspects of making sharp tips. J Vac Sci Technol B 9(2):601–608
34. Eisele M, Krüger M, Schenk M, Ziegler A, Hommelhoff P (2011) Note: Production of sharp gold tips with high surface quality. Rev Sci Instrum 82(2):026101
35. Khan Y, Al-Falih H, Zhang Y, Ng TK, Ooi BS (2012) Two-step controllable electrochemical etching of tungsten scanning probe microscopy tips. Rev Sci Instrum 83(6):063708
36. Choi JW, Hwang GH, Kang SG (2006) Fabrication of a probe needle using a tubular cathode by electrochemical etching. Met Mater Int 12(1):81–84
37. Lee ES (2000) Machining characteristics of the electropolishing of stainless steel (sts316l). Int J Adv Manuf Technol 16(8):591–599
38. Caire JP, Chainet E, Nguyen B, Valenti P (1993) Study of a new electropolishing process for stainless steel tubes. In: American Electroplaters and Surface Finishers Society Conference Proceedings 1993. p 149